$$M{}^{\text{odeling}}_{\text{athematical}}MC{}^{\text{omputing}}$$

Influence of microstructural transformation on quasistatic and dynamic thermomechanical response of thermally loaded disk

Zhuk Y. A.[1], Kashtalyan M.[2]

[1] *Taras Shevchenko National University of Kyiv*
64 Volodymyrska str., 01601, Kyiv, Ukraine
[2] *University of Aberdeen*
Aberdeen AB24 3UE, UK

Within the framework of the dynamic statement of the coupled thermomechanics problem accounting for the microstructural phase transformations invoked by the heating and subsequent cooling of the material, the stress-strains state of the steel disk caused by the thermal pulse is investigated. The axisymmetric problem is solved numerically with application of FEM. Material response is simulated with the use of the thermodynamically consistent theory for inelastic behavior of the material with account of thermal dependencies of physical and mechanical properties. The influence of the microstructural transformations on the dynamic and quasistatic response of the material as well as the residual stress-strain state at the irradiated zone are studied in details.

Keywords: *thermomechanical coupling, microstructural transformation, thermal loading*
2000 MSC: 74, 74F, 74C, 74D, 74F05
UDC: 539.3

1. Introduction

The wide variety of industrial applications of metallic materials is due primarily to the huge range of their mechanical properties and relative simplicity of their modification by various means (grain size refinement, strain hardening, solid solution hardening, etc.) Additional possibilities for property-oriented management are accessible if mechanical and other properties depend on the microstructure of material, which often is a result of specific thermal treatments [1,2].

Laser or electron beam peening has some advantages in comparison with classical techniques for strength, durability and fatigue resistance augmentation (forging, rolling, cogging, etc.) [3]. The length of the laser pulse is easy to manage. Therefore, very short stress pulses can be generated and used as probing signals within the frame of the acoustic defectoscopy technique. Moreover, dosed irradiation by short thermal pulses can be used for surface cleaning, microforming and microforging [1].

There are two main thermomechanical mechanisms of laser pulse influence on a material. Firstly, when a metallic target is irradiated by an intense pulse, the surface layer instantaneously vaporizes into a high temperature and high pressure plasma. This plasma induces shock waves during expansion from the irradiated surface, and mechanical impulses are transferred to the target. This mechanism dominates for the irradiation by the short pulses of high intensity [1,3]. Secondly, the irradiation induces rapid heating with high temperature gradients accompanied by the generation of thermal stresses and shock waves as an inertia effect along with the following gradual cooling. This scenario occurs for prolonged or less intensive pulses. Under these circumstances, the mechanical properties can be changed significantly both on the surface and in the near-surface region resulting in large residual stresses and strains [3–5], which, in turn, can influence the strength, endurance and fatigue life of the structure element. It worth mentioning that this influence can be either positive (enhancing material response in the case of compressive stresses) or negative (compromising structural strength in the case

of tensile stresses). Therefore, the correct prediction of the residual stress-strain state of the structure is of great importance.

Microstructural phase transformations occurring during the heating and subsequent cooling of the material are additional complicating factors affecting the residual state [6–8]. Austenite is the densest of the possible microstructural phases (meanwhile, the specific volume of the martensite is the largest of the all structural phases), and therefore, during the phase transformation upon quenching, there is a net volume increase [9,10]. Consequently, the volume increase upon martensitic transformation is the main cause of straining, distortion, hogging and cracks initiation [6,10].

Dynamic processes generated by the non-steady thermal and mechanical loadings applied to metallic solids possessing fixed microstructural composition were studied in the previous works [3,5]. In the present paper these processes are investigated taking in to account microstructural phase transformations.

It is assumed that during the thermal loading the temperature of the material does not exceed the melting point. To attack the problem, the dynamic problem statement is used [3,5]. The nonlinear material response under complex thermomechanical conditions for wide range of temperature is simulated by the generalized unified Bodner-Partom model [11], which is consistent with the thermodynamics of irreversible processes and is improved to allow for phase transformation [12]. The problem is solved by the finite element method (FEM) technique modified for studying the coupled thermomechanical response of elastic-viscoplastic materials including phase transformations [13]. The influence of the microstructural phase transformation accompanying the heating induced by the thermal pulse and the subsequent cooling on the residual stress-strain state as well as general regularities of coupled thermomechanical and dynamic response of the disk are studied.

2. Model accounting for the microstructural transformations

Generalized thermodynamically consistent modification of the Bodner-Partom model [12] is used to describe the material response under elevated temperatures and high velocity loading [11]. A brief account of the model relations is listed below. It consists of the strain additivity principle: the total strain, ε_{ij}, is representable as a sum of the elastic, ε_{ij}^e, inelastic, ε_{ij}^p, and thermal, ε_{ij}^θ, components (the usual summation convention over the repetitive indices is assumed further on)

$$\varepsilon_{ij} = \varepsilon_{ij}^e + \varepsilon_{ij}^p + \varepsilon_{ij}^\theta, \tag{1}$$

where thermal strain is expressed in the form

$$\varepsilon_{ij}^\theta = \delta_{ij} \int_{\theta_0}^{\theta} \alpha\left(\theta'\right) d\theta'; \tag{2}$$

and θ is a temperature, α is a thermal expansion coefficient; the Hooke's law is written in terms of deviatoric and spherical parts of tensors

$$s_{ij} = 2G\left(e_{ij} - \varepsilon_{ij}^p\right),$$

$$\sigma_{kk} = 3K_V\left(\varepsilon_{kk} - \varepsilon_{kk}^\theta\right), \tag{3}$$

where σ_{ij} and ε_{ij} are the stress and strain tensors, s_{ij} and e_{ij} are the deviators of the stress and strain tensors, and G and K_V are the shear and bulk moduli correspondingly; the flow law along with the condition of plastic incompressibility

$$\dot{\varepsilon}_{ij}^p = \lambda\, s_{ij}, \quad \dot{\varepsilon}_{kk}^p = 0; \tag{4}$$

the kinetic equation

$$D_2^p = D_0^2 \exp\left[-\left(\frac{Z^2}{3J_2}\right)^n\right], \tag{5}$$

where $Z = K + D$, $J_2 = \frac{s_{ij}s_{ij}}{2}$, $D_2^p = \frac{\dot{\varepsilon}_{ij}^p \dot{\varepsilon}_{ij}^p}{2}$, $\lambda^2 = \frac{D_2^p}{J_2}$;

the evolution equations for internal parameters of isotropic, K, and kinematic, β_{ij}, hardening

$$\dot{K} = m_1 \left(K_1 - K\right) \dot{W}_p, \quad K\left(0\right) = K_0, \tag{6}$$

$$\dot{\beta}_{ij} = m_2 \left(D_1 u_{ij} - \beta_{ij}\right) \dot{W}_p, \quad \beta_{ij}\left(0\right) = 0, \tag{7}$$

where $D = \beta_{ij}u_{ij}$, $u_{ij} = \frac{\sigma_{ij}}{\left(\sigma_{ij}\sigma_{ij}\right)^{1/2}}$, $\dot{W}_p = \sigma_{ij}\dot{\varepsilon}_{ij}^p$.

The quantities D_0, D_1, K_0, K_1, m_1, m_2 and n are constants of the model. Theoretical studies and numerous tests [11,12] have shown that the parameters D_0, D_1 and m_2 exhibit weak dependence upon temperature and can be considered to be temperature independent for most metals. Meanwhile, the parameters K_0, K_1, m_1 and n are temperature dependent.

Eqs (6) and (7), in contrast to [11,12], do not contain thermal recovery terms. The processes under consideration here are fast enough to prevent large thermal recovery of taking place.

To describe the microstructural transformations, the following modification of the model Eqs (1)–(7) is proposed. According to Eq. (1), the total strain is expressed as a sum of the elastic, inelastic and thermo-structural, $\varepsilon_{ij}^{\theta s}$, components [13]

$$\varepsilon_{ij} = \varepsilon_{ij}^e + \varepsilon_{ij}^p + \varepsilon_{ij}^{\theta s}, \tag{8}$$

The expressions for the stress and inelastic strain components take the form:

$$\sigma_{ij} = 2G\left(\varepsilon_{ij} - \varepsilon_{ij}^p - \varepsilon_{ij}^{\theta s}\right) + \lambda_E\left(\varepsilon_{kk} - \varepsilon_{kk}^{\theta s}\right)\delta_{ij}, \tag{9}$$

$$\dot{\varepsilon}_{ij}^p = D_0 \exp\left\{-\frac{1}{2}\left[\frac{\left(\bar{K}_0 + K\right)^2}{3J_2}\right]^n\right\}\frac{s_{ij}}{J_2^{1/2}}, \tag{10}$$

$$\varepsilon_{ij}^p\left(0\right) = 0,$$

$$\dot{K} = m_1\left(\bar{K}_1 - K\right)\dot{W}^p, \ K\left(0\right) = 0, \tag{11}$$

where $\bar{K}_0$ and $\bar{K}_1$ are calculated as $\bar{K}_0 = C_\xi K_{\xi 0}$, $\bar{K}_1 = C_\xi K_{\xi 1}$ and λ_E is the Lamй constant, C_ξ are volume concentrations of the microstructural phases, $\xi = f, p, b, m$ for austenite, ferrite, pearlite, bainite and mertensite, respectively; $K_{\xi 0}$ and $K_{\xi 1}$ are parameters of the model for the corresponding phase.

The thermo-structural strain $\varepsilon_{ij}^{\theta s}$ is calculated by making use of the specific volume of the phases V_ξ according to the formula [14]

$$\varepsilon_{ij}^{\theta s}\left(\theta, \theta_r, C_\xi\right) = \frac{V_\xi\left(\theta\right)C_\xi\left(\theta\right) - V_\xi\left(\theta_r\right)C_\xi\left(\theta_r\right)}{3V_\xi\left(\theta_r\right)V_\xi\left(\theta_r\right)}. \tag{12}$$

Here θ is the current temperature and θ_r is some reference temperature.

The temperature dependencies of the specific volumes $V_\xi\left(\theta\right)$ in m³/kg normalized by $\theta = 20°C$ are taken in the form [14]

$$V_a\left(\theta, C_C\right) \cdot 10^3 = 0.12282 + 8.56 \cdot 10^{-6}\left(\theta - 20\right) + 2.15 \cdot 10^{-3}C_C,$$
$$V_{f,p,b}\left(\theta, 20°, C_C\right) \cdot 10^3 = 0.12708 + 5.528 \cdot 10^{-6}\left(\theta - 20\right), \tag{13}$$
$$V_m\left(\theta, 20°, C_C\right) \cdot 10^3 = 0.12708 + 4.448 \cdot 10^{-6}\left(\theta - 20\right) + 2.79 \cdot 10^{-3}C_C,$$

where C_C is the mass percentage of carbon.

Eqs (8)–(13) along with the evolution equation (6) for the parameter of kinematic hardening define the model of the microstructural transformations.

3. Problem statement

The disk of radius R and thickness h is defined in a cylindrical coordinate frame $Orz\varphi$ with $|r| \leqslant R$, $0 \leqslant |z| \leqslant h$. Along with the equations of the response of the material accounting for microstructural transformations given in Section 2, the axisymmetric problem statement contains Cauchy relations between the strain tensor components and the components of the displacement vector $\boldsymbol{u} = (u_r, u_z, u_\varphi)$

$$\varepsilon_z = \frac{\partial u_z}{\partial z}, \quad \varepsilon_r = \frac{\partial u_r}{\partial r}, \quad \varepsilon_\varphi = \frac{u_r}{r},$$
$$\varepsilon_{rz} = \frac{1}{2}\left(\frac{\partial u_z}{\partial r} + \frac{\partial u_r}{\partial z}\right), \tag{14}$$

the equations of motion

$$\frac{\partial \sigma_r}{\partial r} + \frac{1}{r}(\sigma_r - \sigma_\varphi) + \frac{\partial \sigma_{rz}}{\partial z} = \rho\frac{\partial^2 u_r}{\partial t^2},$$
$$\frac{\partial \sigma_{rz}}{\partial r} + \frac{1}{r}\sigma_{rz} + \frac{\partial \sigma_z}{\partial z} = \rho\frac{\partial^2 u_z}{\partial t^2}, \tag{15}$$

the energy balance equation reduced to the heat conduction equation

$$c_v\dot{\theta} + 3\alpha\theta K_V\left(\dot{\varepsilon}_{kk} - 3\alpha\dot{\theta}\right) - D' - k\Delta\theta = r_s, \tag{16}$$

initial conditions

$$u_r = u_z = \dot{u}_r = \dot{u}_z = 0, \quad \theta = \theta_0; \quad t = 0, \tag{17}$$

mechanical boundary conditions

$$\sigma_{ij}n_j = 0 \text{ on } S \tag{18}$$

and appropriate thermal boundary conditions.

The following notation is used in the Eqs (3)–(18): c_v and k are the coefficients of thermal capacity and thermal conductivity, respectively, r_s is the specified intensity of the internal heat sources, D' is the velocity of the mechanical energy dissipation, θ_0 is the initial temperature, n_j are the components of the unit normal on the positive side of the appropriate boundary surface, $\dot{\varepsilon}_{kk} = \dot{\varepsilon}_r + \dot{\varepsilon}_z + \dot{\varepsilon}_\varphi$, $\Delta = \frac{1}{r}\frac{\partial}{\partial r}\left(r\frac{\partial}{\partial r}\right) + \frac{\partial^2}{\partial z^2}$.

The thermal boundary conditions are formulated in a special way to simulate the thermal pulse. The circular region $0 \leqslant r \leqslant r_p$ at the center of the face $z = 0$ is irradiated by the thermal pulse, which is simulated by the heat flow, q_s, through the disk boundary [3,5].

Thermal flow varies according to the rule

$$q_s = \begin{cases} q_0 \cos\dfrac{\pi r}{2r_p}\sin\dfrac{\pi t}{t_p}; & r \leqslant r_p, \ t \leqslant t_p, \\ 0; & r > r_p, \ t > t_p, \end{cases} \tag{19}$$

where t_p is the pulse length and r_p s the radius of heated spot.

Convective heat transfer between the heated spot and the environment is assumed after the completion of the thermal pulse. Herewith, the heat-transfer coefficient is chosen to be high enough, $\alpha_T = 10^5$ kW/m$^2\cdot$K, to simulate the fast forced cooling by means of water shower, cooled gas blasting, etc. This

thermal transfer stops if the temperature at the center of the disk face drops below 50°C. All of the other surfaces of the disk are assumed to be completely insulated from the very beginning.

The effect of the mechanical energy dissipation for impulsive loading was thoroughly studied in the paper [3]. It was found that corresponding temperature increase is less then 10°C. This heating is negligible in comparison to the temperature increase (up to 1300°C) during the pulse. Therefore, temperature effects due to the dissipation of the mechanical energy are negligible for the process under consideration, and the dissipation velocity D' in Eq. (16) can be set to zero.

Eqs (7)–(16) along with initial conditions (17) and boundary conditions (18), (19) provide the statement of coupled thermomechanical problem for inelastic solids under thermal loading accounting for microstructural phase transformations.

4. Solution technique

It is assumed that the disk is made of the steel. The physical and mechanical properties along with the parameters of the Bodner-Partom model for this material as well as their temperature dependencies are taken from the paper [3]. The technique for determining the model parameters over the wide range of temperatures is described in [11] in detail. In the present paper, the microstructure of the material is accounted for through the thermo-structural component Eq. (12) of the total strain, while the dependence of the physical and mechanical properties on the material microstructure is neglected.

The calculation of the concentration of the microstructural phases induced by the transformations of the austenite under temperature decrease is based on the continuous cooling transformation (CCT) diagrams and relations for the specific volumes of the phases Eq. (13). The procedure is described in [2] in detail.

The problem statement Eqs (7)–(19) is intrinsically nonlinear and is attacked numerically. The approach developed initially in [3,5] to solve the dynamic plane or axisymmetric problems of thermo-viscoplasticity is used. It is modified to calculate the microstructural state and the properties of an elementary volume of the disk at each time step.

The numerical solution technique is designed as a double iterative process. The first (internal) process is formed by the numerical integration of the nonlinear system of equations for the material response using an implicit Euler's method. The second iterative process (external) is related to the equation of motion and the integration of the heat conductivity equation. In the frame of this process, the temperature dependencies of the material constants and Bodner-Partom model parameters are taken into account. A time step correction technique is applied to deal with the transition from the elastic to the inelastic response of the material. A simple integration technique is employed for the solution of the nonlinear transcendental system of equations, which arises at each time step. The Steffensen-Eytken technique is used to accelerate the convergence of the process.

The problem is solved using a finite-element technique based on the approach developed in [3,5]. The FEM mesh and the time step are refined to reach 1% of relative accuracy of the stress and inelastic strain intensities, especially in the vicinity of the heating spot to simulate correctly the microstructure of the material and the complex thermomechanical behavior caused by the high temperature gradients.

5. Numerical results and discussion

It is assumed that the disk is made of the steel. The physical and mechanical properties along with the parameters of the Bodner-Partom model for this material as well as their temperature dependencies are taken from the paper [3]. The technique for determining the model parameters over the wide range of temperatures is described in [11] in detail.

In the present paper, the microstructure of the material is accounted for through the thermo-structural component (Eq (12)) of the total strain, while the dependence of the physical and mechanical properties on the material microstructure is neglected.
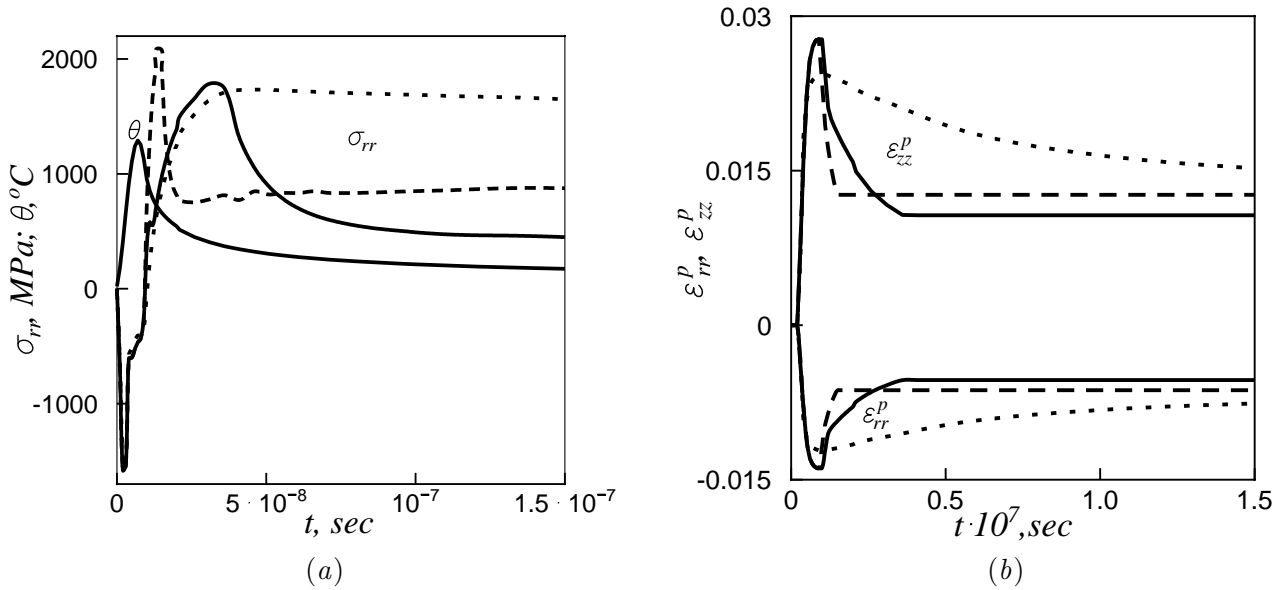
Fig. 1. Evolution of temperature and stress (a) and inelastic strain (b) in the center of the irradiated face.
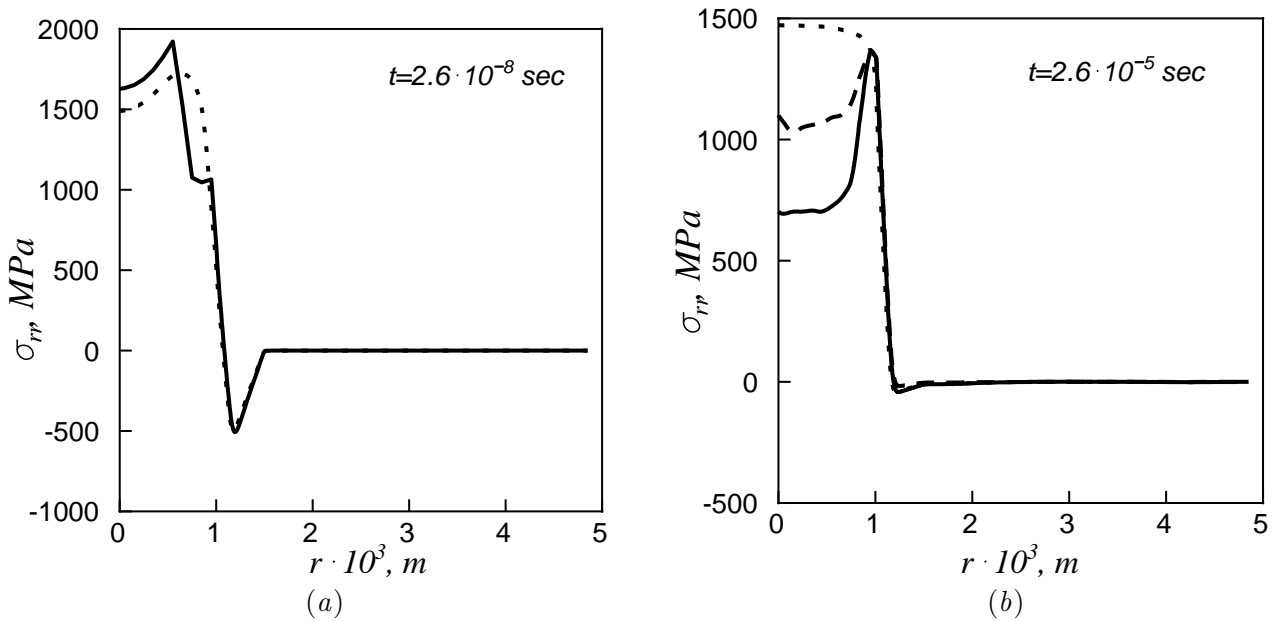

Fig. 2. Evolution of the radial stress distributions along the disk radius.

Calculations were performed for the disk of radius $R = 5 \cdot 10^{-3}$m and thickness $h = 10^{-4}$m. The radius of the heating zone, r_p, was chosen to be equal to $r_p = 1.5 \cdot 10^{-3}$m. The duration of the thermal pulse, t_p, was varied between 10^{-8}sec and 10^{-7}s. Several values of the thermal flow parameter, q_0, lying in the interval between $6 \cdot 10^7$kW/m^2 and $2 \cdot 10^8$kW/m^2 were used. The initial temperature of the disk, θ_0, was equal to 20°C. It is assumed that initial microstructural phase of the disk material is bainite.

Under the irradiation process, the temperature on the disk surface rapidly reaches 1300°C. The heat pulse induces the high temperature gradients in the near-surface region. Then the temperature decreases quite rapidly due to heat propagation inside the disk. There are two scenarios of the development of the process after the completion of the pulse considered in this paper: a) complete thermal insulation of the disk surface, and b) forced cooling of the irradiated spot with high heat-transfer
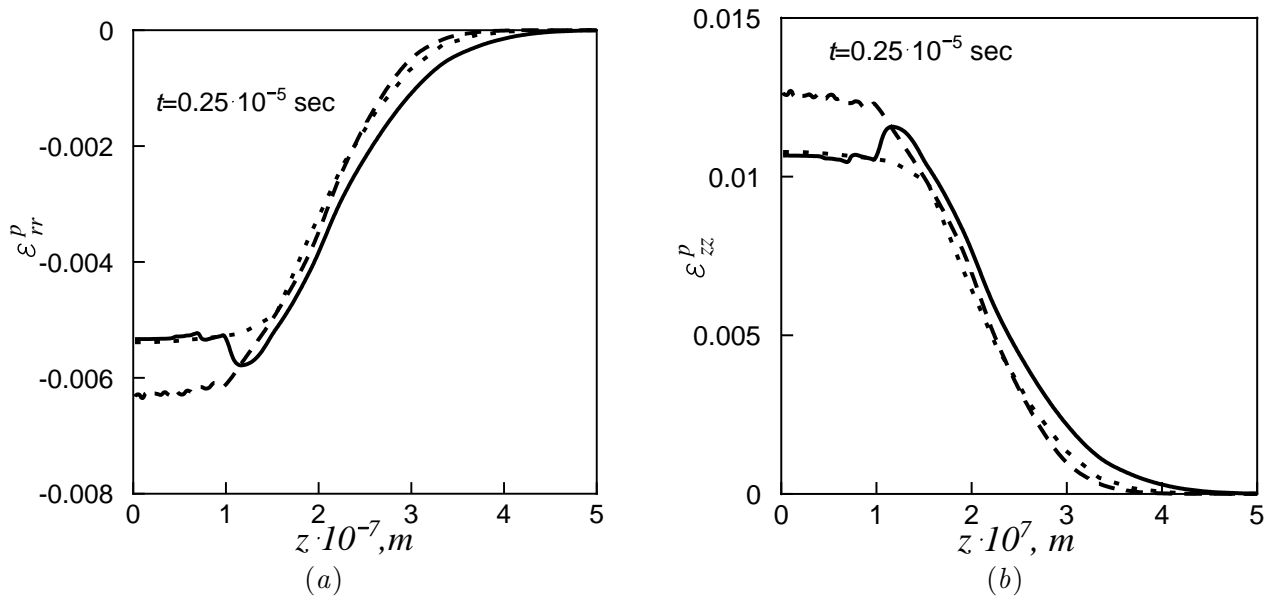
Fig. 3. Spatial distributions of the residual inelastic strains.

coefficient, $\gamma = 10^5$ kW/m^{2}K, provided that all of the other surfaces are still completely insulated. The forced cooling stops as soon as the temperature in the middle of the spot drops below 50°C.

Since the microstructural transformations considered here are temperature induced, the kinetics of the formation of new phases is completely determined by the evolution of the temperature field. It was found that temperature histories obtained under conditions described above for different disk points lead to microstructural transformation bianite–austenite at the heating stage and to transformation austenite-martensite at the cooling stage. As a result, other phases do not appear. For the particular case of forced cooling at $t_p = 10^{-8}$sec and $q_0 = 2 \cdot 10^8$kW/m^2, the origination of the martensitic phase out of the overcooled austenite begins approximately at $t = 1.3 \cdot 10^{-8}$sec. Due to the "bell-like" distribution of the heat flow (see Eq.(19)) along the disk radius, the transformation initially occurs at $r \approx 0.76 \cdot 10^{-3}$m instead of at the center of the spot $r = 0$, $z = 0$.

Under subsequent cooling, the percentage of martensite in the near-surface region gradually increases. This zone expands to the disk axis. When the temperature decreases below the austenite–martensite transformation completion temperature, a region with 100 % martensite content appears. Eventually, a region consisting entirely of the martensite is formed near the center of the disk face, meanwhile all of the surrounding material possesses bainitic microstructure because it was not heated above $A_{C1} = 790$°C. As a result, transformation-induced residual stress-strain state is formed due to the mismatch of the specific volumes of the phases.

Another mechanism contributing to the residual stress-strain state is intensive heating leading to the appearance of inelastic strain. Due to the abrupt material expansion in the irradiated zone, an essential compressive stress occurs inducing the quasistatic component of the stress field. The compressive stresses decrease gradually with time. For times significantly exceeding the pulse length, they change direction and become tensile ones. As a result, a region of tensile residual stresses is formed in the center of the disk face. These effects are demonstrated in Fig. 1. Evolution curves for temperature, θ, and radial stress, σ_{rr}, at the center of the irradiated spot are shown in Fig. 1(a). The dotted line corresponds to the stress obtained as a solution with no phase transformations under a thermally insulated disk surface. The dashed line shows the stress history accounting for the phase transformations under forced cooling, and the solid line – without heat exchange with the surroundings. These curve patterns are preserved everywhere in this paper. It should be pointed out here that the sharp bend in the dashed and solid lines at the initial stage of heating corresponds to microstructural transformation bianite–matrensite occurring when the temperature exceeds the $A_{C1} = 790$°C level.

Same histories for inelastic strain ε_{rr}^p and ε_{zz}^p are shown in Fig. 1(b). They show quite appreciable inelastic strains in the center of the heated spot. Fig. 1(b) shows clearly that neglecting structural transformations leads to an overestimation of the residual stress and strain levels.

Evolution of the radial stress distributions along the disk radius is displayed in Fig. 2. Origination of the martensite possessing the largest possible specific volume induces the increase of the material volume and generation of the stresses, which partly compensate the tension caused by cooling (Fig. 2(a)). This process continues to propagate to the axis of the disk and results in the formation of the final residual stress state (Fig. 2(b)). It is easy to see that the highest level of the residual stress is predicted for the calculations with no accounting for phase transformations. Therefore, the proposed model and calculation technique enables the more precise evaluation of the residual stress-strain state. The lowest level of the potentially damaging residual tensile stresses affecting the material strength is induced under slow gradual cooling. Fast forced cooling causes the opposite effect.

Results for the spatial distributions of the residual inelastic strains are shown in Fig. 3. The typical distributions of ε_{rr}^p along the disk radius (Fig. 3(a)) and the distributions of ε_{zz}^p along the disk thickness (Fig. 3(b)) are displayed there.

The divergence of the curves is observed in the region, which lies within the irradiated zone. Far from the pulse site, the lines are almost coincident.
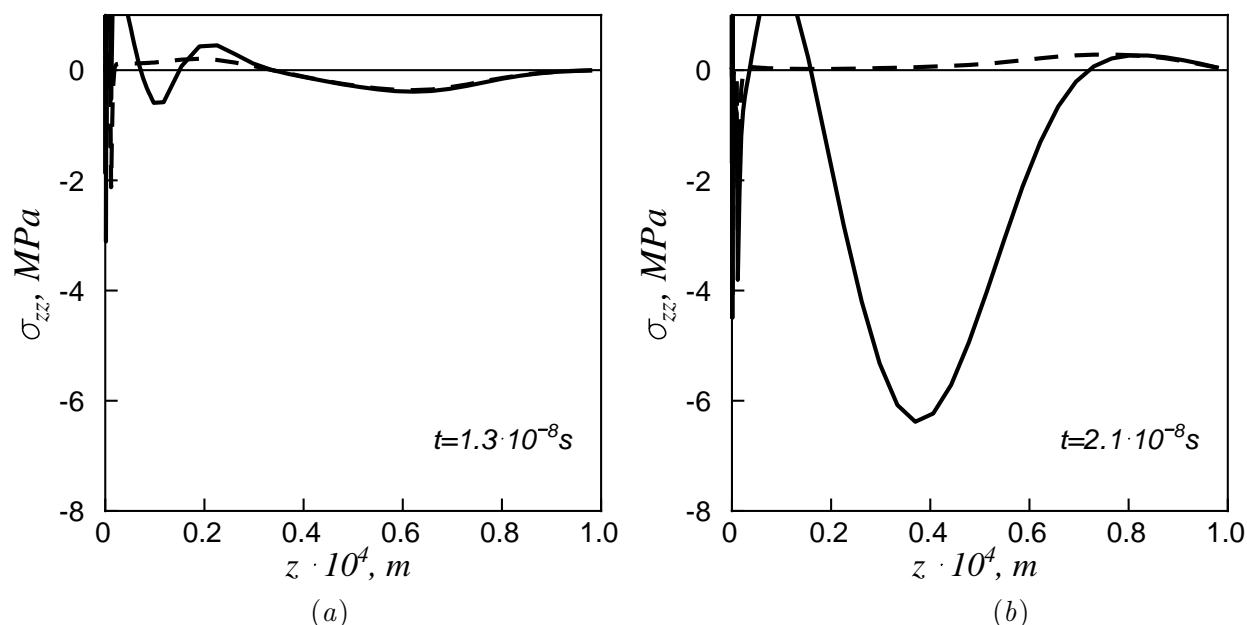

Fig. 4. Comparison of compressive pulses generated due to thermoelastic inertial effects predicted both with account of microstructural transformation and without it.

A stress pulse is generated in the disk as the inertial effect accompanying fast thermoelastic deformation. It represents the dynamic component of stress field, unlike the quasistatic fields considered above. This effect was studied in [5] in detail. Since the method of laser irradiation is applied rather widely in the acoustic technologies of estimating the structure of a material for the generation of a scanning stress pulse, detailed information on this pulse is extremely important. Taking microstructural transformations into account refines substantially the data on this pulse and enables one to improve the technology itself. Indeed, in the case of forced quenching, the formation of a new microstructural phase in supercooled austenite proceeds very rapidly, namely, with the velocity of sound in the material. Hence, in a microscopic volume, martensite is formed practically instantly. Since the specific volume of martensite is the greatest, due to this a compressive pulse is generated. This stress pulse is several tens of times as high as the value of compressive pulse generated due to thermoelastic inertial effects. The results of comparison of such processes is illustrated in Fig. 4.

Here, the solid and dashed lines correspond to the cases of taking microstructural transformations into account under conditions of forced cooling and disregarding these transformations (data from [5] for $t_p = 10^{-8}$ sec, $q_0 = 2 \cdot 10^8$ kW/m^2 and the same geometrical sizes of the disk). We see that the stress pulse caused by austenite-to-martensite microstructural transformation is substantially greater than the thermoelastic pulse, but arises later. The velocity of propagation of both pulses is identical and equal to the velocity of sound in the material.

It is worth noting that this effect is most clearly pronounced for the stress σ_{zz}, which propagates over the disk thickness because a significant part of the material at the center of irradiation zone changes its microstructural state instantly. For the radial stress, the picture turns out very complex and fuzzy as a consequence of the spatial features of microstructural transformation, which are caused by the shape of the irradiation pulse.

6. Conclusions

The proposed technique of the numerical investigation of the coupled thermomechanical problem accounting for the material microstructure enables one to evaluate more precisely the residual stress-strain state of the material below the irradiated site where experimental probing is difficult to perform. The technique is a reliable tool to determine the geometrical dimensions of the pulse affected zone. The approach proposed provides the investigator with the necessary information on the regularities of the residual stress-strain state to find the stress concentration factors and, thus, could be incorporated into fracture prediction techniques developed with the use of the different fracture criteria.

[1] Leblond J. B., Mottet G., Devaux J. C. A theoretical and numerical approach to the plastic behavior of steel during phase transformation. Part 1: Derivation of general relations. J. Mech. Phys. Solids **34**, 395 (1986).

[2] Senchenkov I. K., Zhuk Y. A., Chervinko O. P., Turyk E. Modelling of residual stresses developed in steel cylinders subjected to surface-layer deposition by welding. J. Engrg. Mat. **61**, 271 (2008).

[3] Zhuk Y. A., Senchenkov I. K., Boichuk E. V. Chermomechanical dynamic behavior of a disk subject to an impulsive thermal load at the center. Int. Appl. Mech. **44**, 516 (2008).

[4] Dickey F. M., Holsuade S. C. Laser beam shaping. Theory and techniques. Mavcel Dekker, New York-Basel (2000).

[5] Zhuk Y. A., Senchenkov I. K., Boichuk E. V. Residual stress-strain state of a steel disk under thermal pulsed irradiation. J. Matem. Sci. **160**, 478 (2009).

[6] Nikitin B., Scholtes B., Maier H. J., Altenberger I. High temperature fatigue behavior and residual stress stability of laser shock peened and deep rolled austenitic steel AISI 304. Scripta Mater. **50**, 1345 (2004).

[7] Qin Y., Zou J., Dong C. et al. Temperature-stress fields and related phenomena induced by a high current pulsed electron beam. Nuclear Instrum. Meth. Phys. Research Part B. **225**, 544 (2004).

[8] Valette S., Audouard E., Le Harzic R., et al. Heat affected zone in aluminum single crystals submitted to femtosecond laser irradiations. Appl. Surf. Sci. **239**, 381 (2005).

[9] Chen H., Kysar J., Yao Y. L. Characterization of plastic deformation induced by microscale laser shock peening. J. Appl. Mech. **71**, 713 (2004).

[10] Popov A. A., Popova A. E. Handbook of heat-treater. Isothermal and thermokinetic diagrams for microstructural transformation of the undercooled austenite. GNTI Mashinostroit Lit, Moscow-Sverdlovsk (1961).

[11] Chan K. S., Bodner S. R., Lindholm Phenomenological modeling of hardening and thermal recovery in metals. J. Engng Mater. Technol. **110**, 1 (1998).

[12] Senchenkov I. K., Zhuk Y. A. Thermoviscoplastic deformation of materials. Int. Appl. Mech. **33**, 122 (1997).

[13] Senchenkov I. Thermomechanical model of growing cylindrical bodies made of physically nonlinear materials. Int. Appl. Mech. **41**, 1059 (2005).

[14] Yuriev S. F. Specific Volumes of Phases in the Martensitic Transformation of Austenite. Metallurgizdat, Moscow (1950).

Вплив мікроструктурних перетворень на квазистатичну та динамічну термомеханічну поведінку опроміненого диску

Жук Я. О., Кашталян М.

[1]*Київський національний університет імені Тараса Шевченка*
вул. Володимирська, 64, 01601, Київ, Україна
[2]*Університет Абердіна,*
Абердін AB24 3UE, Великобританія

У рамках динамічної постановки зв'язаної задачі термомеханіки досліджується напружено-деформований стан диска, який виникає внаслідок теплового опромінення, з врахуванням мікроструктурних перетворень, які супроводжують нагрівання і наступне охолодження матеріалу. Розв'язування осесиметричної задачі проводиться чисельно з використанням термодинамічно узгодженої теорії непружної поведінки матеріалу із застосуванням скінченно-елементної методики та врахуванням залежності фізико-механічних властивостей матеріалу від температури. Вивчається вплив мікроструктурних перетворень на динамічну і квазістатичну реакцію матеріалу, а також на залишковий напружено–деформований стан в зоні опромінення.

Ключові слова: *термомеханічна зв'язаність, мікроструктурні перетворення, теплове навантаження*

2000 MSC: 74, 74F, 74C, 74D, 74F05

УДК: 539.3